Measuring the spontaneous curvature of bilayer membranes by molecular dynamics simulations

Han Wang[1,2,*], Dan Hu[3], and Pingwen Zhang[1]

[1] *LMAM and School of Mathematical Sciences, Peking University, Beijing, P.R. China.*
[2] *Institute for Mathematics, Freie Universität Berlin, Berlin, Germany.*
[3] *Department of Mathematics and Institute of Natural Sciences, Shanghai Jiao Tong University, Shanghai, P.R. China*

Abstract. We propose a mathematically rigorous method to measure the spontaneous curvature of a bilayer membrane by molecular dynamics (MD) simulation, which provides description of the molecular mechanisms that cause the spontaneous curvature. As a main result, for the membrane setup investigated, the spontaneous curvature is proved to be a constant plus twice the mean curvature of the membrane in its tensionless ground state. The spontaneous curvature due to the built-in transbilayer asymmetry of the membrane in terms of lipid shape is studied by the proposed method. A linear dependence of the spontaneous curvature with respect to the head-bead diameter difference and the lipid mixing ratio is discovered. The consistency with the theoretical results provides evidence supporting the validity of our method.

Key words: bilayer membrane, Helfrich free energy, spontaneous curvature, molecular dynamics simulation

1 Introduction

A lipid is an amphiphilic molecule that is made up of one hydrophilic head group followed by one or two hydrophobic tails. When lipids are dissolved into a solvent environment, they will self-assemble into various structures, such as micelles, vesicles and bilayers. The lipid bilayer is the basic component of biomembranes that serve as the boundaries of the cells and the organelles, such as the endoplasmic reticulum (ER), the Golgi apparatus and so forth.

The biological functions of cells are closely related to the membrane's shape and the morphological changes. Therefore, in the past decades, a growing interest has been

---

*Corresponding author. *Email addresses:* `han_wang@pku.edu.cn` (H. Wang), `hudan80@sjtu.edu.cn` (D. Hu), `pzhang@pku.edu.cn` (P. Zhang)

drawn to the elastic theory that studies the response of a membrane to the shape deformation [1–4]. One of the most important theories was proposed by Helfrich [1]. It was developed by analogizing to the elastic theory of the liquid crystal. At the continuum level, according to the Helfrich's theory, a membrane is regarded as a fluid elastic sheet, and all atomistic details of the membrane are condensed into three effective parameters: the *bending modulus*, the *spontaneous curvature* and the *Gaussian modulus*. The bending modulus has been extensively studied by experiments [5–9] and molecular simulations [10–14].

The experimental studies have discovered and verified various mechanisms of the spontaneous curvature. Nearly all of them can be summarized into two categories: the bilayer asymmetry and the physical constraint (see [15–18] and the references therein). The bilayer asymmetry can be generated by the transbilayer lipid shape asymmetry [16]. With different kinds of head groups and different numbers of tail chains, the shape of a lipid is analogized to a cone, a cylinder or an inverted cone [19], corresponding to negative, zero or positive spontaneous curvature, respectively. The bilayer asymmetry can also be produced by proteins that insert their hydrophobic parts into one leaflet of the bilayer [20, 21]. The physical constraint stems from the attachment of curved macromolecules to the membrane. For example, if a curved protein is sufficiently rigid and exposes its bent interaction surfaces to the lipid bilayer, a spontaneous curvature is enforced [17, 20, 22–24]. This mechanism is also called protein scaffold.

To precisely measure the spontaneous curvature, a few molecular simulation methods have been developed recently. The pressure profile method has been used to measure the spontaneous curvature of the homogeneous monolayer membrane [25] and protein-membrane complex [26]. This method assumes that the spontaneous curvature can be expressed by the first moment of the bilayer pressure profile. It was pointed out that the pressure profile is not uniquely determined because the expression for the local pressure involves an arbitrary choice of an integration contour [27, 28], though it was also shown that the symmetric part of the pressure tensor is unique under certain conditions [29]. The error of the spontaneous curvature reported by this method is roughly 50% [25, 26]. The spontaneous curvature is also measured by fitting the profile of the curved membrane section to a circle [23, 30]. However, the membrane system is hard to reach equilibrium in a few simulation cases [23, 24]. This method is lack of rigorous theoretical support.

The main purpose of the present paper is to develop a mathematically rigorous method measuring the spontaneous curvature by molecular dynamics (MD) simulation. We first prove the main result of this work: for the system setup investigated in the present paper, the spontaneous curvature is equal to a constant plus twice the mean curvature of a membrane in its tensionless ground state. The constant is eliminated by an antisymmetric system setting, so the spontaneous curvature is measured by the mean curvature. To verify our method, we study the spontaneous curvature induced by the transbilayer lipid shape asymmetry. This case serves as a reference because it has been well studied in the past 20 years [30–38]. In the MD simulations, we adopt an implicit solvent lipid model [10, 39] that is computationally faster comparing with explicit solvent models. To

maintain the antisymmetric configuration during the simulation, the lipid model is modified to prevent the lateral diffusion and flip-flop between the antisymmetric membrane parts. These modifications are shown not to affect the resulting spontaneous curvature and the membrane properties seriously. Finally, a good agreement is achieved by comparing our simulation results with theoretical predictions.

2   Theory

The terminology of spontaneous curvature originates from W. Helfrich's famous work on the elastic properties of lipid bilayers [1]. In the system considered by the present paper (see Fig. 1, details are given in Section 3.2), a piece of membrane is setup in a rectangular periodic simulation box. Two lipid components phase-seperate into two different regions, the boundary between which is always a streight line. Therefore, the geodesic curvature of the phase boundaries vanishes, and followed by the Gauss-Bonnet theorem, the Gaussian curvature contribution is irrelevant. Then the Helfrich free energy reads

$$F = \int \frac{1}{2} \kappa (2H - c_0)^2 \mathrm{d}S, \tag{2.1}$$

where κ is the bending modulus, H is the mean curvature, and c_0 is the spontaneous curvature. It is worthwhile noting that the small curvature assumption is important for Helfrich's theory, so it is to develop our method. This assumption is natural in most biological systems, in which the curvature radius is much larger than the typical membrane thickness (~ 4nm) [16]. However, when the radius of curvature is comparable to or only a few times larger than the membrane thickness, the validity of the Helfrich free energy and our method should be checked carefully. In the large curvature cases, new theories are needed to study the elastic properties. Though the spontaneous curvature c_0 is usually regarded to be homogeneous, it can be inhomogeneous as a matter of fact. For example, proteins such as the clathrin and adaptin can induce local bending of a membrane [40]. In the case study of this work, lipids of different shapes phase separate into different regions, as a result, the spontaneous curvature c_0 is a function of the position.

We consider a membrane that expands in a periodic simulation box and reaches its tensionless ground state, which means the equilibrium state without internal tension and external force. The coordinate of the membrane is denoted by its height above the reference plane $z = 0$ ("Monge gauge"), namely $h(x,y)$. The spontaneous curvature profile is thereby denoted by $c_0(x,y)$. Note that this description will fail when large deformation happens, for example, when the membrane puckers up. The dimension of the periodic simulation box is denoted by $L_x \times L_y \times L_z$. Its projected region on the reference plane (namely $[0,L_x] \times [0,L_y]$) is denoted by Ω. In all the simulations, the y dimension of the box L_y is fixed. The free energy, as a function of the membrane shape and the box size L_x, is denoted by $F[h,L_x]$. When the deformation is small, the mean curvature of the membrane can be linearly approximated by $H(x,y) = \frac{1}{2}\Delta h(x,y)$, so the free energy is ap-

proximately

$$F[h,L_x] = \int_\Omega \frac{1}{2}\kappa [\Delta h(x,y) - c_0(x,y)]^2 \mathrm{d}x\mathrm{d}y. \tag{2.2}$$

If the free energy is first order differentiable with respect to the box size, the tension free condition yields

$$-\frac{\partial F}{\partial L_x}\bigg|_{L_x=\hat{L}_x} = 0. \tag{2.3}$$

We will use this condition to determine the box size. Since the membrane is incompressible, the change of the box size L_x will result in a change of the membrane shape h, which suggests L_x is a functional of h. Under the tension free condition, we have the following equation for the equilibrium state:

$$\frac{\delta F}{\delta h}\bigg|_{h=\hat{h}} + \frac{\partial F}{\partial L_x}\bigg|_{L_x=\hat{L}_x} \cdot \frac{\delta L_x}{\delta h} = \frac{\delta F}{\delta h}\bigg|_{h=\hat{h}} = 0$$
$$\Rightarrow \quad \kappa \Delta [\Delta \hat{h}(x,y) - c_0(x,y)] = 0. \tag{2.4}$$

Where $\hat{h}$ denotes the coordinate of the membrane in the equilibrium state. Solving equation (2.4) with periodic boundary condition gives

$$\Delta \hat{h}(x,y) = c_0(x,y) - \frac{1}{|\Omega|}\int_\Omega c_0(x,y)\mathrm{d}x\mathrm{d}y, \tag{2.5}$$

or equivalently

$$c_0(x,y) = 2H(x,y) + \frac{1}{|\Omega|}\int_\Omega c_0(x,y)\mathrm{d}x\mathrm{d}y. \tag{2.6}$$

If the system is set up properly so that the integral term $\frac{1}{|\Omega|}\int_\Omega c_0(x,y)\mathrm{d}x\mathrm{d}y$ vanishes, then we have $c_0(x,y) = 2H(x,y)$, and the spontaneous curvature is obtained by measuring the mean curvature. We would like to point out that the above resutl is not necessarily correct for other system setup.

The mean curvature is only well-defined for a smooth membrane, which is at least second order differentiable. However, in the MD simulations, the membrane is very rough due to both the presence of thermal fluctuation and the discrete nature of the lipids. Below we describe how to obtain the smoothed profile on a rectangular mesh. First the $x-y$ reference plane is divided into small bins. Then the averaged height of the mass center of the lipids in a bin is used to define the height of the smooth membrane at the center of the bin (mesh point). All derivatives of the membrane are calculated by finite differences. The coordinate and the derivatives are time-averaged to eliminate the thermal fluctuation.

3   Testing case: the spontaneous curvature due to the transbilayer lipid shape asymmetry

3.1   The solvent free lipid model

We adopt the solvent-free lipid model developed by I.R. Cooke, M. Deserno and K. Kremer [39]. A lipid is coarse grained into three connected beads, one bead representing the hydrophilic head group, followed by two beads representing the hydrophobic tail(s). No explicit solvent bead exists, because the hydrophobic interaction between the solvent and the tail beads is effectively represented by a long-range attractive interaction between the tail beads. The physical properties of Cooke model fall in the experimental interesting range, except for the flip-flop rate [10].

The size of the beads is defined by the repulsive Weeks-Chandler-Anderson potential,

$$V_{\text{rep}}(r) = \begin{cases} 4\epsilon \left[\left(\frac{b}{r}\right)^{12} - \left(\frac{b}{r}\right)^{6} + \frac{1}{4} \right], & r \leq r_c \\ 0, & r > r_c. \end{cases} \tag{3.1}$$

Where $r_c = 2^{1/6}b$ is the cutoff of the repulsive core. ϵ is the unit of the energy. The head-head and head-tail non-bonded interactions are of this kind with a typical setting $b = 0.95\sigma$, where σ is the unit of the length. The non-bonded interaction between tail beads is the Weeks-Chandler-Anderson potential plus a cosine-shaped long range attractive tail:

$$V_{\text{cos}}(r) = \begin{cases} -\epsilon & r < r_c, \\ -\epsilon \cos^2 \left[\frac{\pi}{2} \left(\frac{r - r_c}{w_c} \right) \right] & r_c \leq r \leq r_c + w_c, \\ 0 & r > r_c + w_c. \end{cases} \tag{3.2}$$

The typical diameter of the tail beads is $b_{tail} = \sigma$, and the range of the attractive tail is controlled by the parameter $w_c = 1.6\sigma$. With the aforementioned parameters, the lipids self assemble to a fluid state bilayer membrane at $k_B T = 1.08\epsilon$, although $1\% - 2\%$ of the lipids reside in the gas phase surrounding the bilayer [10]. Actually, the lipids self-assemble to the fluid state bilayer membrane in a wide parameter range, and that is why the Cooke model is highly tunable (see the phase diagram in Ref. [10]).

The beads are connected by the finite extensible nonlinear elastic (FENE) bond interaction:

$$V_{\text{bond}}(r) = -\frac{1}{2} k_{\text{bond}} r_{\infty}^2 \log \left[1 - \left(\frac{r}{r_{\infty}} \right)^2 \right], \tag{3.3}$$

with a magnitude $k_{\text{bond}} = 30\epsilon/\sigma^2$, and a maximum stretching length $r_{\infty} = 1.5\sigma$. A harmonic bending interaction between the head bead and the second tail bead is applied to keep the lipids straight, saying

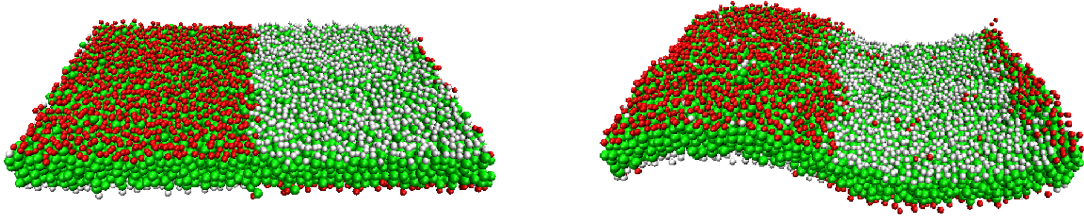$$V_{\text{bend}} = \frac{1}{2} k_{\text{bend}} (r - r_0)^2, \tag{3.4}$$

Figure 1: Snapshots of a typical testing system. The testing system consists of a periodic box of size $57.208\sigma \times 40\sigma \times 60\sigma$, containing 4160 lipids, one-half of which are of type A (lipids with white head group) and the other half are of type B (lipids with red head group). All tail beads are shown in green. The head group difference is $\alpha = 0.1\sigma$. The system is coupled with a velocity rescaling thermostat to provide a canonical sampling at temperature $k_B T = 1.08\epsilon$. The configurations of the system at $t = 0\tau$ (left) and $t = 500,000\tau$ (right) are presented.

with a bending stiffness $k_{\text{bend}} = 10\epsilon/\sigma^2$, and an equilibrium length $r_0 = 4\sigma$.

3.2 System settings

The testing system (see Fig. 1) consists of two lipids species, namely type A (lipids with white head and green tail) and type B (lipids with red head and green tail). The diameters of the head beads are denoted by $b_A = 0.95\sigma - 0.5\alpha$ and $b_B = 0.95\sigma + 0.5\alpha$, respectively. The parameter α represents the geometric difference between the two types of head beads. The two types of lipids have the same tail beads. A flat membrane parallel to the x–y plane is initially set up in a periodic simulation box, in which the two types of lipids are perfectly separated (see Fig. 1). The upper monolayer on the left-half is made up of lipid B, while the lower monolayer is made up of lipid A. The right-half of the membrane is set up in an opposite way . The x–y positions of the lipids are randomly generated. The integral of the spontaneous curvature $\frac{1}{|\Omega|}\int_\Omega c_0(x,y)\,dxdy$ vanishes due to this antisymmetric system configuration. According to equation (2.6), the spontaneous curvature is directly obtained from the mean curvature. Obviously, only half of the lipid coordinates are sufficient in calculating the spontaneous curvature due to the antisymmetry, and it is possible to modify the boundary condition to reduce the computational cost. However, to make sure the testing simulations fit for most MD packages that only provide standard boundary conditions, the periodic boundary condition is adopted.

The typical in-plane diffusion rate is of order $10^{-2}\sigma^2/\tau$. In our simulations that are typically as long as $5 \times 10^5\tau$, the molecules of the left- and right-half will mix up. To avoid this entropy driven mixture, we modify the tail interaction parameter w_c between the molecules of the left- and right-half of the membrane. More precisely, a cosine-shape tail potential with a shorter attractive range is used: $w_c^{\text{LR}} = 1.48\sigma < w_c$. It has been shown [41] that this modification will lead to a phase separation between lipids A and B. The ratio of lipid B in the A-rich phase is under 3% in our testing simulations. Unfortunately, there exists a tension along the border between the two phases, which implies the tension free condition is not perfectly satisfied. However, the line tension is along the y direction, so it

will not affect the bending of the membrane along the x direction. Therefore, when coupling the system to a barostat that conducts the zero-tension simulation, the y dimension of the simulation box is fixed, and the x dimension is adjusted to fulfill the tension free condition. To test the side effect of the line tension, we increase w_c^{LR} from 1.48σ to 1.50σ in a testing system of $\alpha = 0.1\sigma$. The resulting line tension decreases from $1.91\epsilon/\sigma$ to $1.08\epsilon/\sigma$, while the measured spontaneous curvature increases from $0.044\sigma^{-1}$ to $0.046\sigma^{-1}$, only by 5%. Therefore, the side effect due to the line tension is not serious.

The flip-flop rate of the Cooke model is much higher than the experimental value [10]. This is generally a good property, because the system equilibrates much faster. In our testing systems, it is undesirable because the upper and lower monolayers will mix up by the intermonolayer flip-flops. To eliminate this mixture, the cosine-shaped tail interaction (3.2) between the middle beads of lipids in the upper and lower monolayer is once and for all turned off, even when a lipid flips to the opposite leaflet, the attractive tail will NOT be truned on. Therefore, the flip-floped state is energetically less favorable. As a result, in the ground tensionless state, the ratio of the flip-flopped lipids is below 1%. Since the typical distance between the middle beads (3σ) is larger than the cutoff radius of the attractive interaction (2.72σ), the lipids cannot feel the change of the interaction when they do not try to flip-flop. This modification will not disturb the following properties of the bilayer too much: the area per lipid changes from $1.20\sigma^2$ to $1.16\sigma^2$; the thickness of the bilayer changes from 5.32σ to 5.50σ. The change of the bending modulus (measured by analyzing the membrane's Fourier mode spectrum [10]) is relatively bigger: from $14.8k_BT$ to $21.5k_BT$, but it will not enter Eqn. (2.6). The spontaneous curvature of the membrane may also be disturbed, and unfortunately, it is not easy to analyze this side-effect. It is worthwhile noting that the modification is only designed for the Cooke model, the flip-flop rate of which is much higher than the experimental value. For most of the explicit solvent models and some implicit solvent models (e.g. [42]), the flip-flop event is rarely observed in the typical timescale of simulation, so the modification is not necessary.

We further measure the spontaneous curvature of the membrane composed by a mixture of lipids A and B, and study how the spontaneous curvature changes as a function of the mixing ratio. The system is set up in the following way: the lower monolayer of the left-half is composed by lipid A of ratio ρ and lipid B of ratio $1-\rho$, with all lipids randomly mixed; the upper monolayer is composed by lipid B of ratio ρ and lipid A of ratio $1-\rho$. The right-half is set up in the antisymmetric way. The tail interactions are modified in the aforementioned way to maintain the mixing ratio.

3.3 Theoretical results

It is argued [37] that the spontaneous curvature can be expressed by the lipid molecular packing parameter, V/Sl, where V is the volume of the entire lipid molecular, l is the length of lipid, and S is the area of the head group. The spontaneous curvature in the

case of a relaxed cylindrical monolayer, is given by

$$\bar{c}_0^X = \frac{2}{l_X}\left(\frac{V_X}{S_X l_X} - 1\right), \quad X = A, B, \tag{3.5}$$

for the lipid type A and B, respectively. A bar is added on $\bar{c}_0^X$ to distinguish the monolayer spontaneous curvature from the bilayer spontaneous curvature. For the lipid model used in the present paper, it is reasonable to assume

$$V_X = C_v b_X^3 + D_v b_{tail}^3, \tag{3.6}$$

$$l_X = C_l b_X + D_l b_{tail}, \tag{3.7}$$

$$S_X = C_s b_X^2, \tag{3.8}$$

where C_v, C_l, C_s, D_v and D_s are constants. The spontaneous curvature of a bilayer is related to the spontaneous curvature of the upper ($\bar{c}_0^u$) and lower ($\bar{c}_0^l$) monolayer by

$$c_0 = \frac{1}{2}(\bar{c}_0^u - \bar{c}_0^l). \tag{3.9}$$

By using (3.5) – (3.9), it can be shown that the spontaneous curvature of the lipid bilayer is proportional to α that is the head bead diameter difference between the upper and lower monolayer.

In the case of lipid A and B mixture, theoretical analysis as well as experimental results have shown that the spontaneous curvature can be reasonably approximated by the linear combination of the components' spontaneous curvatures with a weight of the mixing ratio [31, 32, 37], saying

$$\bar{c}_0^l = \rho \bar{c}_0^A + (1-\rho)\bar{c}_0^B, \tag{3.10}$$

$$\bar{c}_0^u = (1-\rho)\bar{c}_0^A + \rho \bar{c}_0^B. \tag{3.11}$$

Equation(3.9) – (3.11) yield the spontaneous curvature of the mixed bilayer:

$$c_0 = \left(\rho - \frac{1}{2}\right)(\bar{c}_B - \bar{c}_A), \tag{3.12}$$

which linearly depends on the mixing ratio ρ.

3.4 Simulation details and results

Typically, a flat membrane composed of 4160 lipids is initially set up in a $60\sigma \times 40\sigma \times 60\sigma$ simulation box with the periodic boundary condition. First, a simulation varying the box dimension L_x is performed to fulfill the tension free condition on x direction. This is achieved by coupling the system to a Berendsen barostat [43]. At the same time, the temperature of the system is controlled to $k_B T = 1.08\epsilon$ by a Berendsen thermostat [43]. The system is integrated by the leap frog scheme with a time step of 0.005τ. When the
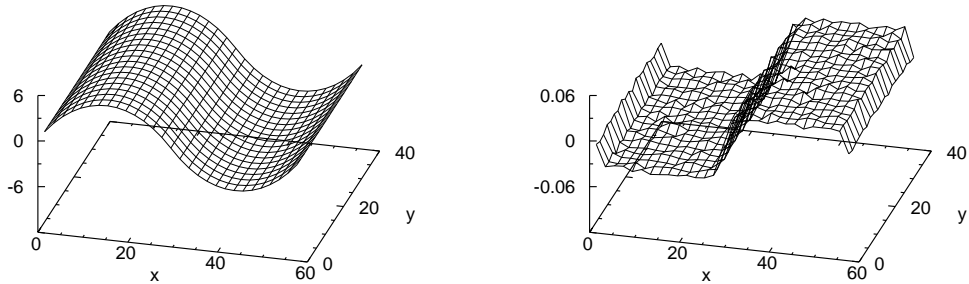
Figure 2: The continuous membrane (left) and the spontaneous curvature profile (right) constructed from the lipid coordinates. The unit of x and y axis is σ. The unit of the membrane profile is σ and the unit of the spontaneous curvature is σ^{-1}.

system is equilibrated, the average box dimension $\hat{L}_x$ is calculated. Then a NVT system composed of the same amount of lipids is set up in a $\bar{L}_x \times 40\sigma \times 60\sigma$ simulation box. The velocity Verlet method is used to integrate with a time step of 0.005τ. The velocity rescaling thermostat [44] is used to provide a canonical sampling at the same temperature $k_B T = 1.08\epsilon$. The time scale of the thermostat is τ. The system is evolved form 0τ to $500{,}000\tau$ and is fully equilibrated after $50{,}000\tau$. We sample the coordinates of lipids as well as other quantities of interest from $t_{\text{start}} = 100{,}000\tau$ to $t_{\text{end}} = 500{,}000\tau$ with a time interval of $\Delta t = 10\tau$.

We first show the results of the testing system of head bead difference $\alpha = 0.1\sigma$. Calculated from the coordinates of lipids, the profile of the smoothed membranes and the spontaneous curvature are presented in Fig. 2. The $x-y$ plane is approximately divided into small bins of size $\sigma \times \sigma$. We observe the phase interface is fixed and the normal direction (or the tangential plane) are continuous across the interfaces. Moreover, the Gaussian modulus are the same for the membrane phases due to the antisymmetric setup. Therefore, the Gaussian curvature doesn't contribute in determining the equilibrium shape of the membrane. The spontaneous curvature profiles show relatively constant regions on the left- and right-half membrane. This is because the lipid compositions of the left- and right-half membrane are homogeneous. The constant spontaneous curvature value of the left-half is opposite to that of the right-half, owing to the antisymmetry. Therefore, the information in the spontaneous curvature profile can be reduced into a positive constant value that defines the global spontaneous curvature due to the transbilayer lipid shape asymmetry. We also observe a transition region of roughly 10σ between the left- and right-half membrane. From this point of view, the size of the simulation box on the x direction should be no less than 40σ.

The spontaneous curvature due to the lipid shape asymmetry should be independent with the size of the system. To verify this point, we measured the spontaneous curvatures of the following three system settings: 1388 lipids in a $40\sigma \times 20\sigma \times 60\sigma$ box, 4160 lipids in
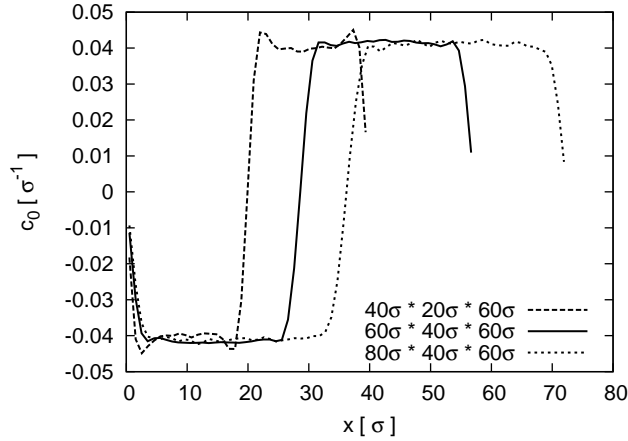
Figure 3: The spontaneous curvature profiles of three systems of different sizes: 1388 lipids in a $40\sigma \times 20\sigma \times 60\sigma$ box, 4160 lipids in a $60\sigma \times 40\sigma \times 60\sigma$ box and 5548 lipids in a $80\sigma \times 40\sigma \times 60\sigma$ box. The head bead difference is $\alpha = 0.1\sigma$.

a $60\sigma \times 40\sigma \times 60\sigma$ box, and 5548 lipids in a $80\sigma \times 40\sigma \times 60\sigma$ box. The head bead differences are the same: $\alpha = 0.1\sigma$. The spontaneous curvature profiles are plotted in Fig. 3, with data averaged on y direction for clarity. The resulting spontaneous curvatures (constant values of the profiles) of the 4160 lipids system and the 5548 lipids system are almost the same. The value of the 1388 lipids system is a little smaller and the profile presents two abnormal peaks at the transition region. Therefore, we adopt the 4160 lipids system that calculates the right spontaneous curvature with comparatively small computational cost.

In section 3.3, we theoretically demonstrated that the spontaneous curvature depends linearly on the head bead difference α. If our method is valid, this linear dependence should be preserved. We measure and present in Fig. 4 the spontaneous curvature as a function of the head group difference α. The spontaneous curvature is calculated by averaging the constant value region of the spontaneous curvature profile. The error bar presents the standard deviation of the averaged data. The figure shows perfect linear relationship in range $\alpha \in [0, 0.2\sigma]$. An α bigger than 0.2 will not lead to an equilibrium bilayer membrane, because pores form at the contact line between the left- and right-half. The spontaneous curvature at $\alpha = 0.2\sigma$ is $0.088\sigma^{-1}$, corresponding to the curvature of a spherical vesicle of radius 11σ. The MD length unit σ can be mapped to a real length of 0.7 nm to 1.0 nm [10], so the real size of the vesicle is 7.7 nm to 11 nm, which is much smaller than those found in the intracellular membrane transport (radii ~ 30 nm) [16]. Therefore, our method work in a considerably large range of the spontaneous curvature that covers the experimentally interesting region.

In the case of lipid A and B mixture, the spontaneous curvature as a function of the mixing ratio is plotted in Fig. 5. Several head bead differences are considered: $\alpha = 0.04\sigma$, 0.08σ, 0.12σ, 0.16σ and 0.20σ. A good linear growth of the spontaneous curvature with respect to the mixing ratio is presented, which is consistent with the theoretical
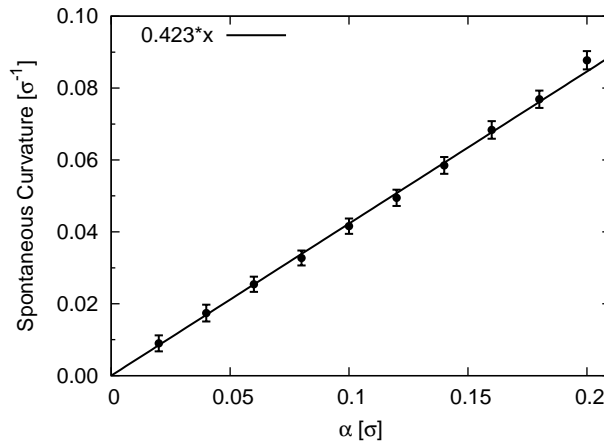
Figure 4: The spontaneous curvature as a function of head group difference α. The solid line with a slope of $0.423\sigma^{-2}$ is the linear fitting to the data points. The error bars denote the standard deviations of the sampled values.

prediction, i.e. Eqn. (3.12). The slopes of the linear growth (straight lines in Fig. 5) are predicted from Fig. 4, where the mixing ratio $\rho = 1.0$. A good consistency with the data points is observed.

4 Conclusions and remarks

In this paper, we proposed a mathematically rigorous method to measure the spontaneous curvature of a bilayer membrane by the molecular dynamics simulation. The method was verified by a case study: measuring the spontaneous curvature due to the transbilayer lipid shape asymmetry.

As a main result, for the system setup investigated, the spontaneous curvature was shown to be a constant plus twice of the mean curvature, when the membrane is in its tensionless ground state. In the case study, the system was set up in an antisymmetric configuration to eliminate the constant in the spontaneous curvature – mean curvature relation (2.6). To maintain this antisymmetry in the native state, the lipid model was elaborately modified to prevent the lateral diffusion and flip-flop between the antisymmetric membrane parts. To measure the spontaneous curvature precisely, we sampled and averaged 4×10^4 mean curvature profiles on the MD trajectory. The resulting spontaneous curvature was found to be independent with the size of the simulation box, when the system is sufficiently large. A linear dependence with respect to the head bead difference as well as the mixing ratio of two types of lipid components was discovered. This relationship is consistent with the theoretical prediction in a considerable large range. The good agreement is a strong evidence supporting the validity of our method.

The proposed method can be used the study other origin of spontaneous curvature. In the case of the protein scaffolding, the spontaneous curvature measured by the present
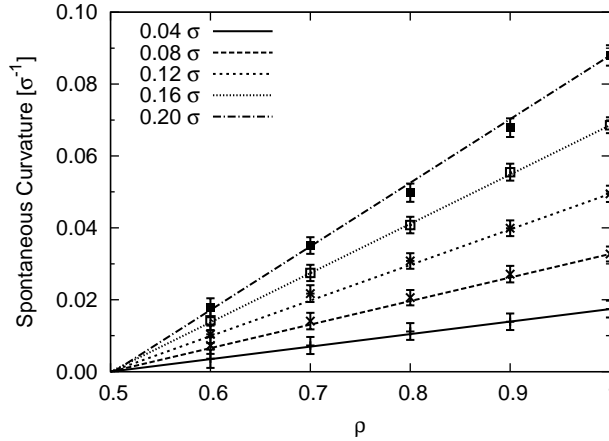
Figure 5: The spontaneous curvature as a function of the mixing ratio ρ. Several head bead differences are considered: $\alpha = 0.04\sigma$, 0.08σ, 0.12σ, 0.16σ and 0.20σ. The lines indicate the slopes predicted from Fig. 4. The error bars denote the standard deviations of the sampled values.

method is the "global spontaneous curvature", which is a long-time averaged curvature induced by the scaffolding protein, rather than the local curvature instantaneously forced by the protein. Therefore, the time scale of the simulation should be noticeably longer than the typical time scale required for a protein to diffuse the distance between two proteins.

Acknowledgment

References

[1] W. Helfrich. Elastic properties of lipid bilayers: theory and possible experiments. *Z Naturforsch [C]*, 28(11):693–703, 1973.

[2] D.J. Steigmann. On the relationship between the cosserat and kirchhoff-love theories of elastic shells. *Mathematics and Mechanics of Solids*, 4(3):275–288, 1999.

[3] R. Capovilla, J. Guven, and J.A. Santiago. Deformations of the geometry of lipid vesicles. *Journal of Physics A: Mathematical and General*, 36:6281–6295, 2003.

[4] D. Hu, P. Zhang, and W. E. Continuum theory of a moving membrane. *Physical Review E*, 75(4):41605, 2007.

[5] F. Brochard and J.F. Lennon. Frequency spectrum of the flicker phenomenon in erythrocytes. *Journal de Physique*, 36(11):1035–1047, 1975.

[6] J.F. Faucon, M.D. Mitov, P. Meleard, I. Bivas, and P. Bothorel. Bending elasticity and thermal fluctuations of lipid membranes. theoretical and experimental requirements. *Journal de Physique*, 50(17):2389–2414, 1989.

[7] E. Evans and W. Rawicz. Entropy-driven tension and bending elasticity in condensed-fluid membranes. *Physical Review Letters*, 64(17):2094–2097, 1990.

[8] W. Rawicz, K.C. Olbrich, T. McIntosh, D. Needham, and E. Evans. Effect of chain length and unsaturation on elasticity of lipid bilayers. *Biophysical Journal*, 79(1):328–339, 2000.

[9] D. Cuvelier, I. Derényi, P. Bassereau, and P. Nassoy. Coalescence of membrane tethers: experiments, theory, and applications. *Biophysical Journal*, 88(4):2714–2726, 2005.

[10] I.R. Cooke and M. Deserno. Solvent-free model for self-assembling fluid bilayer membranes: Stabilization of the fluid phase based on broad attractive tail potentials. *The Journal of Chemical Physics*, 123:224710, 2005.

[11] R. Goetz, G. Gompper, and R. Lipowsky. Mobility and elasticity of self-assembled membranes. *Physical Review Letters*, 82(1):221–224, 1999.

[12] V.A. Harmandaris and M. Deserno. A novel method for measuring the bending rigidity of model lipid membranes by simulating tethers. *The Journal of Chemical Physics*, 125:204905, 2006.

[13] E. Lindahl and O. Edholm. Mesoscopic undulations and thickness fluctuations in lipid bilayers from molecular dynamics simulations. *Biophysical Journal*, 79(1):426–433, 2000.

[14] S.J. Marrink and A.E. Mark. Effect of undulations on surface tension in simulated bilayers. *Journal of Physical Chemistry B*, 105(26):6122–6127, 2001.

[15] H.T. McMahon and J.L. Gallop. Membrane curvature and mechanisms of dynamic cell membrane remodelling. *Nature*, 438:590–596, 2005.

[16] J. Zimmerberg and M.M. Kozlov. How proteins produce cellular membrane curvature. *Nature Reviews Molecular Cell Biology*, 7(1):9–19, 2005.

[17] A. Frost, V.M. Unger, and P. De Camilli. The bar domain superfamily: membrane-molding macromolecules. *Cell*, 137(2):191–196, 2009.

[18] M.M. Kozlov. Biophysics: Joint effort bends membrane. *Nature*, 463(7280):439, 2010.

[19] C. Hamai, T. Yang, S. Kataoka, P.S. Cremer, and S.M. Musser. Effect of average phospholipid curvature on supported bilayer formation on glass by vesicle fusion. *Biophysical Journal*, 90(4):1241–1248, 2006.

[20] P.D. Blood, R.D. Swenson, and G.A. Voth. Factors influencing local membrane curvature induction by n-bar domains as revealed by molecular dynamics simulations. *Biophysical Journal*, 95(4):1866–1876, 2008.

[21] F. Campelo, H.T. McMahon, and M.M. Kozlov. The hydrophobic insertion mechanism of membrane curvature generation by proteins. *Biophysical Journal*, 95(5):2325–2339, 2008.

[22] P.D. Blood and G.A. Voth. Direct observation of bin/amphiphysin/rvs (bar) domain-induced membrane curvature by means of molecular dynamics simulations. *Proceedings of the National Academy of Sciences*, 103(41):15068, 2006.

[23] A. Arkhipov, Y. Yin, and K. Schulten. Four-scale description of membrane sculpting by bar domains. *Biophysical Journal*, 95(6):2806–2821, 2008.

[24] A. Arkhipov, Y. Yin, and K. Schulten. Membrane-bending mechanism of amphiphysin n-bar domains. *Biophysical Journal*, 97(10):2727–2735, 2009.

[25] S.J. Marrink, H.J. Risselada, S. Yefimov, D.P. Tieleman, and A.H. de Vries. The martini force field: coarse grained model for biomolecular simulations. *Journal of Physical Chemistry B*, 111(27):7812–7824, 2007.

[26] O.H.S. Ollila, H.J. Risselada, M. Louhivuori, E. Lindahl, I. Vattulainen, and S.J. Marrink. 3D

pressure field in lipid membranes and membrane-protein complexes. *Physical Review Letters*, 102(7):78101, 2009.

[27] P. Schofield and J.R. Henderson. Statistical mechanics of inhomogeneous fluids. *Proceedings of the Royal Society of London. Series A, Mathematical and Physical Sciences (1934-1990)*, 379(1776):231–246, 1982.

[28] F. Varnik, J. Baschnagel, and K. Binder. Molecular dynamics results on the pressure tensor of polymer films. *The Journal of Chemical Physics*, 113:4444, 2000.

[29] E. Wajnryb, A.R. Altenberger, and J.S. Dahler. Uniqueness of the microscopic stress tensor. *Journal of Chemical Physics*, 103(22):9782–9787, 1995.

[30] A.J. Markvoort, R.A. van Santen, and P.A.J. Hilbers. Vesicle shapes from molecular dynamics simulations. *Journal of Physical Chemistry B*, 110(45):22780, 2006.

[31] R.P. Rand, N.L. Fuller, S.M. Gruner, and V.A. Parsegian. Membrane curvature, lipid segregation, and structural transitions for phospholipids under dual-solvent stress. *Biochemistry*, 29(1):76–87, 1990.

[32] S. Leikin, M.M. Kozlov, N.L. Fuller, and R.P. Rand. Measured effects of diacylglycerol on structural and elastic properties of phospholipid membranes. *Biophysical Journal*, 71(5):2623–2632, 1996.

[33] N. Fuller and R.P. Rand. The influence of lysolipids on the spontaneous curvature and bending elasticity of phospholipid membranes. *Biophysical Journal*, 81(1):243–254, 2001.

[34] E.E. Kooijman, V. Chupin, B. de Kruijff, and K.N. Burger. Modulation of membrane curvature by phosphatidic acid and lysophosphatidic acid. *Traffic*, 4(3):162–174, 2003.

[35] J.N. Israelachvili, D.J. Mitchell, and B.W. Ninham. Theory of self-assembly of hydrocarbon amphiphiles into micelles and bilayers. *Journal of the Chemical Society, Faraday Transactions 2*, 72:1525–1568, 1976.

[36] J.N. Israelachvili, D.J. Mitchell, and B.W. Ninham. Theory of self-assembly of lipid bilayers and vesicles. *Biochimica et Biophysica Acta*, 470(2):185, 1977.

[37] D. Marsh. Intrinsic curvature in normal and inverted lipid structures and in membranes. *Biophysical Journal*, 70(5):2248–2255, 1996.

[38] I.R. Cooke and M. Deserno. Coupling between lipid shape and membrane curvature. *Biophysical Journal*, 91(2):487, 2006.

[39] I.R. Cooke, K. Kremer, and M. Deserno. Tunable generic model for fluid bilayer membranes. *Physical Review E*, 72(1):11506, 2005.

[40] B. Alberts, D. Bray, A. Johnson, J. Lewis, M. Raff, K. Roberts, P. Walter, and A.M. Campbell. *Essential Cell Biology*. Garland Science New York, 2004.

[41] B.J. Reynwar and M. Deserno. Membrane composition-mediated protein-protein interactions. *Biointerphases*, 3:FA117–FA124, 2008.

[42] A.J. Sodt and T. Head-Gordon. An implicit solvent coarse-grained lipid model with correct stress profile. *The Journal of Chemical Physics*, 132:205103, 2010.

[43] H.J.C. Berendsen, J.P.M. Postma, W.F. Van Gunsteren, A. DiNola, and J.R. Haak. Molecular dynamics with coupling to an external bath. *The Journal of Chemical Physics*, 81:3684, 1984.

[44] G. Bussi, D. Donadio, and M. Parrinello. Canonical sampling through velocity rescaling. *The Journal of Chemical Physics*, 126:014101, 2007.